Nanoscale

Accepted Manuscript

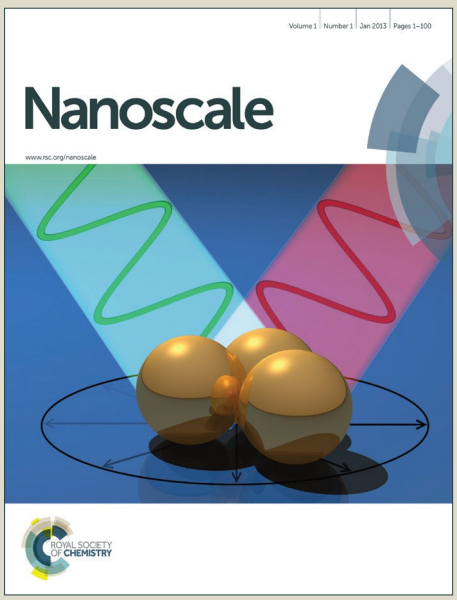

ROYAL SOCIETY OF CHEMISTRY

www.rsc.org/nanoscale

Nanoscale

PAPER

A Degradable Polydopamine Coating Based on Disulfide-Exchange Reaction

Received 00th January 20xx,
Accepted 00th January 20xx

DOI: 10.1039/x0xx00000x

www.rsc.org/

Daewha Hong,[a] Hojae Lee,[a] Beom Jin Kim,[a] Taegyun Park,[a] Ji Yu Choi,[a] Matthew Park,[a] Juno Lee,[a] Hyeoncheol Cho,[a] Seok-Pyo Hong,[a] Sung Ho Yang,[b] Sun Ho Jung,[c] Sung-Bo Ko,[c] and Insung S. Choi*[a]

Although the programmed degradation of biocompatible films finds its applications in various fields including biomedical and bionanotechnological areas, the coating methods have generally been limited to be substrate-specific, not applicable to any kinds of substrates. In this paper, we report a dopamine derivative, which allows for both universal coating of various substrates and stimuli-responsive film degradation, inspired by mussel-adhesive proteins. Two dopamine moieties are linked together by the disulfide bond, the cleavage of which enables the programmed film degradation. Mechanistic analysis of the degradable films indicates that the initial cleavage of the disulfide linkage causes a rapid uptake of water molecules, hydrating the films, which leads to rapid degradation. Our substrate-independent coating of degradable films would provide an advanced tool for drug delivery systems, tissue engineering, and anti-fouling strategies.

Introduction

Polydopamine-based, substrate-independent coating,[1] inspired by the adhesive property of mussels in nature, has intensively been used in various fields, ranging from biomedicine to energy-related fields.[2,3] Its extraordinary adhesion property, presumably stemming from the synergistic effects of 1,2-hydroxybenzene (catechol) and amine groups, has led 2-(3,4-dihydroxyphenyl)ethylamine (dopamine) as a minimal building block to coat virtually all substrates, including superhydrophobic surfaces,[4-6] electrodes,[7,8] and even living cell surfaces.[9,10] Moreover, the derivatization of dopamine also has provided the additional or orthogonal functionalities that expanded the characteristics and applications of the coated surfaces.[11-18] For example, the polymerization and cross-linking of 6-nitrodopamine produced photocleavable and self-healing matrices.[14] The polydopamine derivative films that possessed *o*-methylphenyl aldehyde moieties were used for the attachment of external biomolecules via photo-triggered Diels-Alder reaction.[15] Norepinephrine, having an additional OH group, has been proposed as an ultrasmooth coating unit,[16] and its β-OH group allowed for additional functions, such as a site for ring-opening polymerization.[17] We also have recently reported the use of a perfluorinated dopamine derivative for self-cleaning, superhydrophobic coating on various substrates.[18] Although the processability of dopamine has proved multifunctionally useful toward various surfaces, the formation of polydopamine-based, degradable films remains elusive, because the high adhesiveness is generally not compatible with degradability.

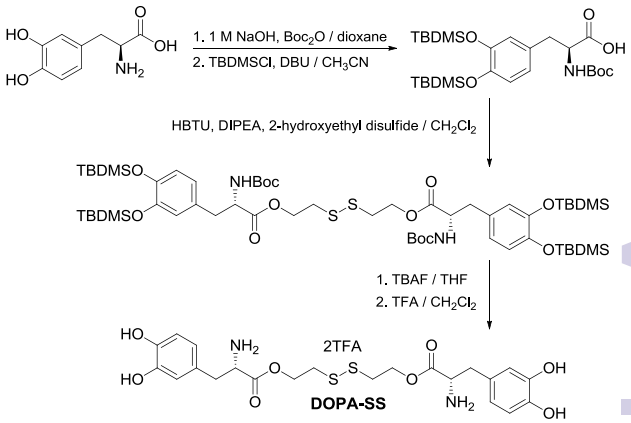

Fig. 1 Synthesis of DOPA-SS. Boc_2O: di-*tert*-butyl dicarbonate; TBDMSCl: *tert*-butyldimethylsilyl chloride; DBU: 1,8-diazabicyclo[5.4.0]undec-7-ene; DIPEA: *N,N*-diisopropylethylamine; TBAF: tetrabutylammonium fluoride; TFA: trifluoroacetic acid; HBTU: *N,N,N′,N′*-tetramethyl-*O*-(1*H*-benzotriazol-1-yl)uronium hexafluorophosphate.

Stimulus-responsive, degradable coating offers basic but indispensable tools for drug delivery systems, tissue engineering, cosmetics, and anti-fouling strategies. For example, spatiotemporal release and subsequent delivery of therapeutics to target tissues are achieved by controlled degradation of drug-embedding cargos.[19-21] The non-specific adsorption of marine-bio mass onto vessel surfaces also would be eliminated by degradable coating.[22] In addition, recent interest has been focused on degradable cell-surface engineering to manipulate cellular metabolism and activities

[a] *Center for Cell-Encapsulation Research, Department of Chemistry, KAIST, Daejeon 305-701, Korea, E-mail: ischoi@kaist.ac.kr*
[b] *Department of Chemistry Education, Korea National University of Education, Chungbuk 363-791, Korea*
[c] *Medigen, Inc., Daejeon 305-811, Korea*
† Electronic Supplementary Information (ESI) available: Synthesis, characterization, and other additional details. See DOI: 10.1039/x0xx00000x

a single-cell level.[23,24] However, degradable films have mainly been formed by layer-by-layer (LbL) assembly[25-27] and surface-initiated polymerization,[28,29] which require substrate-specific chemical interactions between a substrate and coating materials. Although it was reported that the LbL procedure could be made substrate-independent with pre-coating of catechol derivatives,[30,31] it is still highly demanding to develop a method for the universal and degradable coating. In this work, we designed a dopamine derivative that formed stimulus-responsive, degradable films on virtually any substrates.

Results and discussion

We used 3,4-dihydroxy-L-phenylalanine (L-DOPA) as a starting material in our synthetic design, because the dopamine moiety kept preserved with derivatization of the carboxyl group (Fig. 1).[18,32] After protection of the hydroxyl and amine groups in L-DOPA, two dopamine structures were linked together by the disulfide (S-S) bond, which would be broken to two thiol (SH) groups under reducing conditions. The subsequent deprotection reactions generated a water-soluble dopamine derivative, denoted as DOPA-SS in this paper, and the coating was performed under slightly basic conditions (pH 8.5) at room temperature.

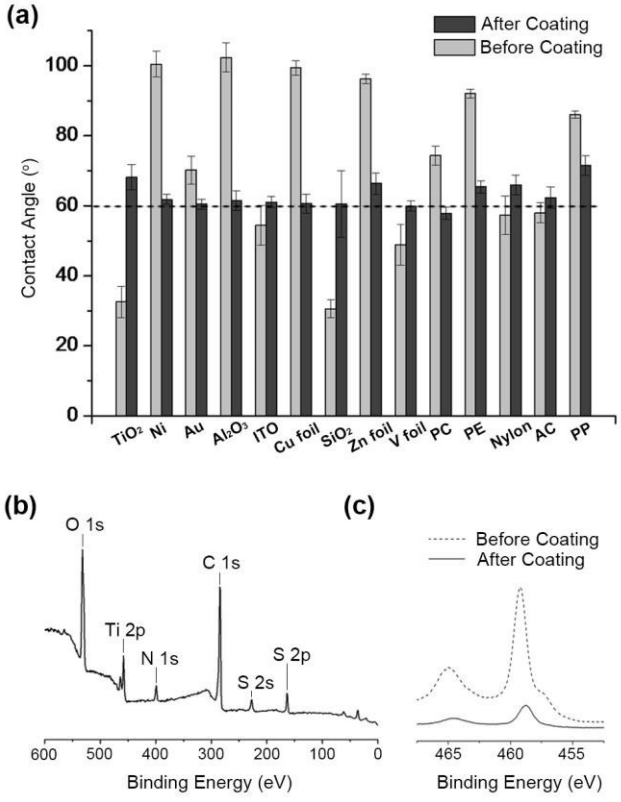

Fig. 2 Characterizations of DOPA-SS films. (a) Static water contact angles of the substrates before (gray) and after (black) DOPA-SS film formation. (b) Wide-scan XPS spectrum of DOPA-SS-coated TiO_2. (c) The Ti(2p) region of the XPS spectra of bare and DOPA-SS-coated TiO_2.

We coated various surfaces, such as titanium oxide (TiO_2), nickel (Ni), gold (Au), aluminum oxide (Al_2O_3), indium tin oxide (ITO), copper foil (Cu foil), silicon oxide (SiO_2), zinc foil (Zn foil), vanadium foil (V foil), polycarbonate (PC), polyethylene (PE), nylon, acryl plate (AC), and polypropylene (PP). The coating proved substrate-independent: after coating the water contact angles of all the samples tested converged to about 60° regardless of the initial values that were significantly variable depending upon the identity of the substrates. (Fig. 2a). The X-ray photoelectron spectroscopy (XPS) analysis also confirmed the successful coating. For example, the XPS spectrum of the TiO_2 substrate showed the characteristic peaks of DOPA-SS at 399.6 (N 1s), 227.8 (S 2s), and 164.9 eV (S 2p) (Fig. 2b, see ESI, Fig. S1† for the XPS spectra of the other substrates). The C(1s) XPS peak was deconvoluted to obtain further information on the coated film: the peaks appearing at 285.9 and 289.0 eV corresponded to the C-X (X = O, N, or S) and the C=O bond, respectively, confirming the existence of the functional group of DOPA-SS (see ESI, Fig. S2†). In contrast, the signal intensities of TiO_2 (Ti $2p_{3/2}$, 458.7 eV; $2p_{1/2}$, 464.7 eV) decreased significantly after coating, indicating that the DOPA-SS film attenuated the characteristic signals of the underlying TiO_2 substrate (Fig. 2c). The ellipsometric thickness of the DOPA-SS film was measured to be 27.5 nm for TiO_2.

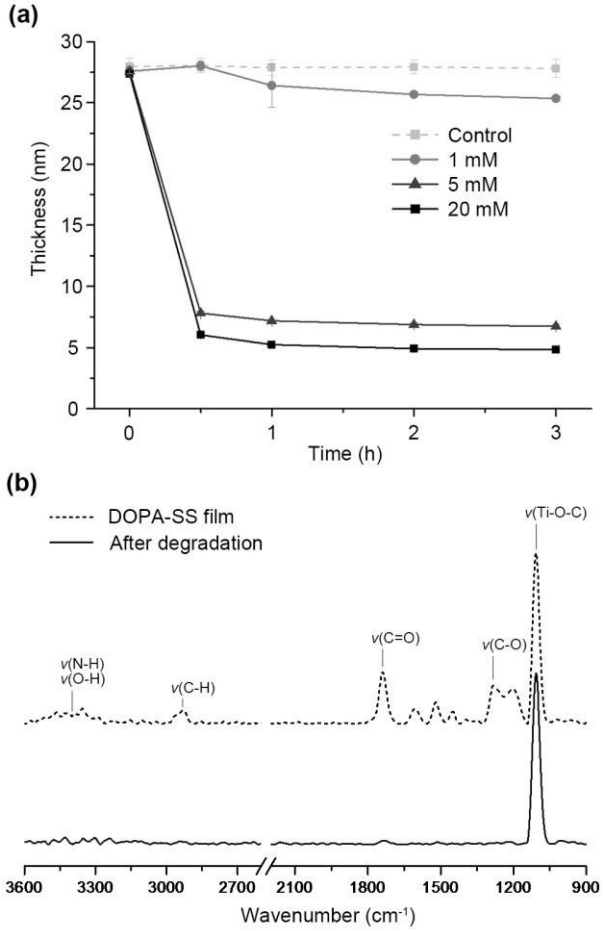

Fig. 3 (a) Graphs of DOPA-SS film thickness *vs.* time with different concentrations of GSH. (b) FT-IR spectra of the DOPA-SS films before and after degradation (20 mM of GSH, 1 h).

The degradation characteristics of the DOPA-SS film were investigated with glutathione (GSH) as a reducing agent,

intracellular antioxidant that prevents cell damages by reducing reactive oxygen species.[33] We chose the GSH concentrations of 1, 5, and 20 mM, because the substantial difference in the GSH concentration between inner (~10 mM) and exterior (~2 μM) cells in this range[34] has been utilized for the controlled release of drug in the target cells.[35,36] The DOPA-SS film degradation, monitored by the ellipsometric measurements, was found to be concentration-dependent (Fig. 3a). The 1 mM of GSH had a negligible effect on degradation compared with a control (Tris, pH 7.4), but higher concentrations of GSH (5 mM and 20 mM) led to fast film degradation. The XPS peaks from TiO_2 (Ti $2p_{3/2}$, 458.7 eV; $2p_{1/2}$, 464.7 eV) were recovered after GSH treatment, which additionally supported the removal of the DOPA-SS film from the TiO_2 substrate (see ESI, Fig. S3†). The Fourier-transform infrared (FT-IR) spectra showed the chemical states of the DOPA-SS films before and after degradation (Fig. 3b). The peaks from DOPA-SS at 3500-3300 (ν(N-H) and ν(O-H)), 2930 (ν(C-H)), 1739 (ν(C=O)), and 1282 and 1204 cm^{-1} (ν(C-O)) were barely observed after treatment of GSH (20 mM; 1 h), while the peak at 1107 cm^{-1} (ν(Ti-O-C))[37] remained unchanged. In addition, the characteristic peaks of the indole structure[38] at 1606 (ν_{ring}(C=C)), 1520 (ν_{ring}(C=N)), and 1606 cm^{-1} (ν_{ring}(CNC)) were not observed after degradation. The IR results indicated that the film was removed except for the adlayer that was covalently linked with TiO_2.

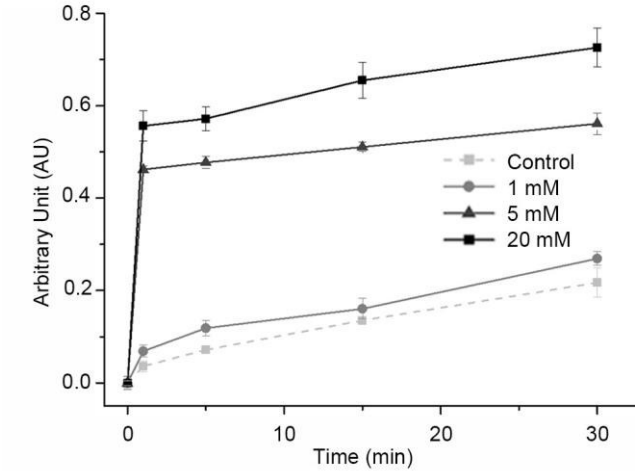

Fig. 4 Release of doxorubicin from the DOPA-SS film in the presence of GSH.

As a proof-of-concept demonstration for controlled drug release systems, we co-deposited a therapeutic, doxorubicin, with DOPA-SS, and investigated its release behaviors with GSH as a reducing agent. Fluorescence spectrometry analysis showed the concentration-dependent release profiles of doxorubicin (Fig. 4). When the concentration of GSH was 5 mM or 20 mM, doxorubicin was released mostly in 1 min, and reached a plateau after 30 min. In contrast, 1 mM of GSH and the control (Tris pH 7.4 without GSH) showed a passive release of doxorubicin. Doxorubicin-free DOPA-SS films showed a negligible fluorescence signal, indicating that the degraded components of DOPA-SS films did not interfere with the detection of doxorubicin (data not shown).

To investigate mechanistic details of the film degradation process over time, quartz crystal microbalance with dissipation (QCM-D) experiments were conducted. In Fig. 5, the change in frequency (Δf) and dissipation (ΔD) represented the state of the mass change and film viscoelasticity, respectively, upon GSH addition to an adsorbed DOPA-SS film.[39-41]

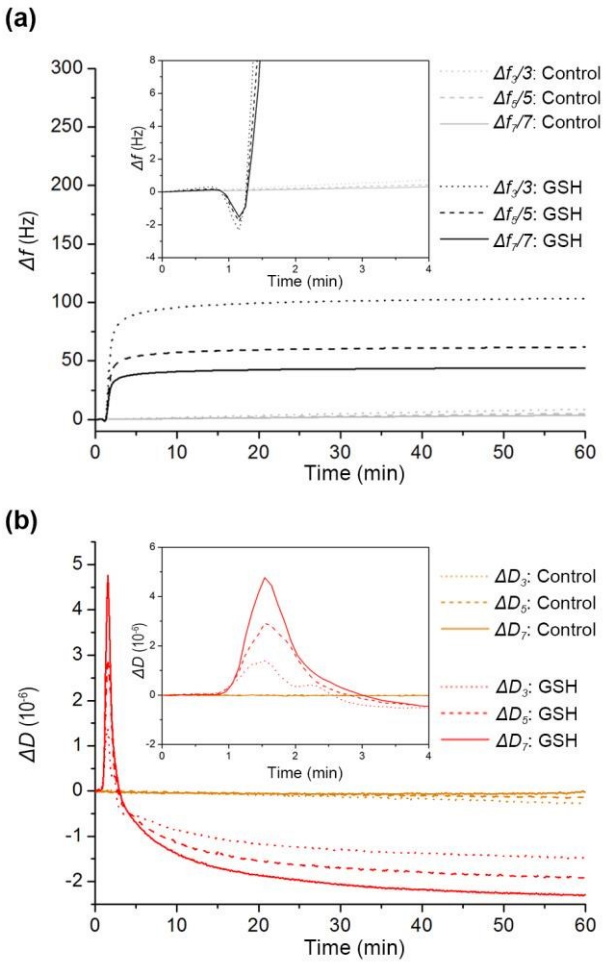

Fig. 5 QCM-D spectra of the DOPA-SS-coated TiO_2. (a) Normalized frequency change ($\Delta f_n/n$) where n is the odd overtone integer and (b) energy dissipation change (ΔD) as functions of time were measured after the injection of GSH (20 mM). Simultaneous measurements were recorded at three overtones (n=3, 5, and 7).

Almost immediately, a sharp increase in frequency ($\Delta f > 0$) was observed with the injection of 20 mM GSH, which was indicative of a rapid mass decrease at the surface layer (Fig. 5a). Of interest is the observation that the dissipation increased sharply ($\Delta D > 0$) with a decrease in frequency ($\Delta f < 0$) right after injection of GSH, and it gradually decreased with the increase in frequency (Fig. 5b). Based on the QCM-D data, we believed that the introduction of GSH to the DOPA-SS film induced the initial decrease in the degree of crosslinking by reducing the S-S bond to the SH groups, which led to increase in hydration mass ($\Delta f < 0$, frequency decrease) and in the corresponding film viscoelasticity ($\Delta D > 0$, energy dissipation increase) at the very early stage of degradation.[42,43] The relatively high degree of hydration (as indicated by the ΔD/Δf ratio) would subsequently increase the accessibility of GSH

which in turn enabled the rapid degradation of the DOPA-SS films within a short period of time. Simultaneously, the spread between the three experimentally measured overtones (n=3, 5, and 7) increased dramatically (Fig. 5b), indicating that the physical characteristics of the DOPA-SS films changed from a rigid layer to a soft, viscoelastic layer during the initial stage of the degradation process. In contrast, the DOPA-SS films without GSH (control) showed negligible changes in Δf and ΔD, supporting that the degradation of the DOPA-SS films was caused by GSH, which cleaved the disulfide network. In addition, negligible differences in Δf and ΔD were observed for the 1 mM GSH solution compared with a control, while the 5 mM GSH solution led to lower mass decrease than the 20 mM GSH solution, which was consistent with the ellipsometric analysis (see ESI, Fig. S4†).

Conclusions

In summary, we reported the substrate-independent coating of degradable polydopamine that contained the disulfide linkage. We believe that our work showed several advantages in the area of functional thin films: (1) on-demand degradability with universality: many technologically important applications, including drug delivery systems, frequently require the controlled degradation of materials and films in response to external stimuli. The formation of degradable films is also highly demanded to be universal, not requiring substrate-specificity, exemplified by a metal-organic film of ferric ion and tannic acid.[44] Our work clearly adds the important property of controlled degradability to the polydopamine films, while preserving their universality of coating; (2) cytocompatibility: the cytocompatible degradability of the DOPA-SS films is highly advantageous for various biomedical applications, such as drug delivery systems, tissue engineering, and cell therapy, where the intimate contact between living cells and coating materials is required. Our system also could be applied to cell surface engineering, where the controlled formation and degradation of films should be performed in a cytocompatible fashion;[45] (3) design flexibility: it is possible to develop various building blocks of coating for certain applications by incorporating additional functionalities of interest to L-DOPA.

Experimental Section

Film formation and degradation

All substrates were washed thoroughly with ethanol before coating processes. The buffer solution (10 mM Tris, pH 8.5) of DOPA-SS (2.5 mM) was prepared and carefully poured over a substrate for coating. After 3 h, the substrate was washed with DI water and dried under a stream of argon gas. The substrate was coated again with a freshly prepared Tris solution of DOPA-SS for 3 h, and washed with DI water, and dried under a stream of argon gas. The buffer solution (10 mM Tris, pH 7.4) of GSH (1, 5, or 20 mM) was used for DOPA-SS film degradation. DOPA-SS-coated substrates were immersed in the prepared GSH solution for predetermined time, washed with DI water, and dried under a stream of argon gas.

Release profiles of doxorubicin

The buffer solution (10 mM Tris, pH 8.5) of DOPA-SS (2.5 mM) and doxorubicin hydrochloride (125 μM) was prepared, and carefully poured over TiO_2 substrates for coating. After 3 h, the TiO_2 substrates were washed with DI water and dried under a stream of argon gas. For GSH-mediated film degradation and release of doxorubicin, the substrates were incubated in a buffer solution (10 mM Tris, pH 7.4) of GSH (1, 5, or 20 mM) for predetermined time. An aliquot was taken from the solution, and its fluorescence intensity was measured by fluorescence spectrometry (λ_{ex} = 480 nm; λ_{em} = 580 nm) for the quantification of released doxorubicin.

QCM-D analysis of DOPA-SS-coated films

Quartz crystal microbalance with dissipation (QCM-D) measurements for frequency change, Δf, and dissipation change, ΔD, were performed with a Q-sense E4 system (Biolin Scientific). A titanium-coated crystal was used (Biolin Scientific). Tris buffered solution (10 mM, pH 7.4) was used as a flow (flow rate: 50 μL/min). The DOPA-SS-coated crystal was mounted at room temperature and prewashed with a buffer solution for 20 min. The degradation of the DOPA-SS films was performed by injecting the buffer solution that contained GSH (20 mM), and time-course changes in the Δf and ΔD were measured simultaneously at the seven different overtones for 1 h. The crystal was excited at its fundamental frequency (5 MHz), and the measurements were performed at the first, third, fifth, seventh, ninth, eleventh, and thirteenth overtones, corresponding to 5, 15, 25, 35, 45, 55, and 65 MHz, respectively. For the analysis, Δf and ΔD of the third, fifth, and seventh overtone of a QCM crystal were used.

Characterizations

All synthesized compounds were characterized by nuclear magnetic resonance spectroscopy (NMR, Inova) operated at the ultrashield of 400 MHz. High resolution mass spectrometry (HR-MS, Bruker Daltonik) was used for the characterization of DOPA-SS. The X-ray photoelectron spectroscopy (XPS) study was performed with a VG-Scientific spectrometer (model Sigma Prove) with a monochromatized Al Kα X-ray source (1486.6 eV). Emitted photoelectrons were detected by a multi-channel detector at a take-off angle of 90° relative to the surface. During the measurements, the base pressure was 8.0 × 10^{-8} Torr. Survey spectra were obtained at a resolution of 1 eV from 2 scans, and high-resolution spectra were acquired at a resolution of 0.05 eV from 15 scans. Contact angle measurements were performed with Phoenix 300 apparatus (Surface Electro Optics Co.) equipped with a video camera. The static contact angles of 2-μL water droplets were measured at more than five different locations on each sample, and the average values were reported in this paper. The fluorescence intensities of doxorubicin (λ_{ex} = 480 nm; λ_{em} = 580 nm) were measured with a Varioskan Flash Multimode Reader (Ther

Scientific). The thickness of the DOPA-SS films was measured with a Gaertner L116s ellipsometer (Gaertner Scientific Corporation) equipped with a He-Ne laser (632.8 nm) at a 70° angle of incidence. A refractive index of 1.46 was used for all the films. FT-IR spectra were obtained in vacuum with an IFS-66v/S FTIR spectrometer (Bruker).

Acknowledgements

This work was supported by the Basic Science Research Program through the National Research Foundation of Korea (NRF) funded by the Ministry of Science, ICT & Future Planning (MSIP) (2012R1A3A2026403)

References

1 H. Lee, S. M. Dellatore, W. M. Miller and P. B. Messersmith, *Science*, 2007, **318**, 426-430.
2 Y. Liu, K. Ai and L. Lu, *Chem. Rev.*, 2014, **114**, 5057-5115.
3 M. d'Ischia, A. Napolitano, V. Ball, C.-T. Chen and M. J. Buehler, *Acc. Chem. Res.*, 2014, **47**, 3541-3550.
4 I. You, S. M. Kang, S. Lee, Y. O. Cho, J. B. Kim, S. B. Lee, Y. S. Nam and H. Lee, *Angew. Chem. Int. Ed.*, 2012, **51**, 6126-6130.
5 S. M. Kang, I. You, W. K. Cho, H. K. Shon, T. G. Lee, I. S. Choi, J. M. Karp and H. Lee, *Angew. Chem. Int. Ed.*, 2010, **49**, 9401-9404.
6 D. Hong, I. You, H. Lee, S.-g. Lee, I. S. Choi and S. M. Kang, *Bull. Korean Chem. Soc.*, 2013, **34**, 3141-3142.
7 K. Kang, S. Lee, R. Kim, I. S. Choi and Y. Nam, *Angew. Chem. Int. Ed.*, 2012, **51**, 13101-13104.
8 K. Kang, I. S. Choi and Y. Nam, *Biomaterials*, **2011**, *32*, 6374-6380.
9 S. H. Yang, S. M. Kang, K.-B. Lee, T. D. Chung, H. Lee and I. S. Choi, *J. Am. Chem. Soc.*, 2011, **133**, 2795-2797.
10 B. Wang, G. Wang, B. Zhao, J. Chen, X. Zhang and R. Tang, *Chem. Sci.*, 2014, **5**, 3463-3468.
11 C. M. Preuss, M. M. Zieger, C. Rodriguez-Emmenegger, N. Zydziak, V. Trouillet, A. S. Goldmann and C. Barner-Kowollik, *ACS Macro Lett.*, 2014, **3**, 1169-1173.
12 C. M. Preuss, A. S. Goldmann, V. Trouillet, A. Walther and C. Barner-Kowollik, *Macromol. Rapid Commun.*, 2013, **34**, 640-644.
13 B. P. Lee, J. L. Dalsin and P. B. Messersmith, *Biomacromolecules*, 2002, **3**, 1038-1047.
14 Z. Shafiq, J. Cui, L. Pastor-Pérez, V. S. Miguel, R. A. Gropeanu, C. Serrano and A. del Campo, *Angew. Chem. Int. Ed.*, 2012, **51**, 4332-4335.
15 C. M. Preuss, T. Tischer, C. Rodriguez-Emmenegger, M. M. Zieger, M. Bruns, A. S. Goldmann and C. Barner-Kowollik, *J. Mater. Chem. B*, 2014, **2**, 36-40.
16 S. Hong, J. Kim, Y. S. Na, J. Park, S. Kim, K. Singha, G.-I. Im, D.-K. Han, W. J. Kim and H. Lee, *Angew. Chem. Int. Ed.*, 2013, **52**, 9187-9191.
17 S. M. Kang, J. Rho, I. S. Choi, P. B. Messersmith and H. Lee, *J. Am. Chem. Soc.*, 2009, **131**, 13224-13225.
18 D. Hong, K. Bae, S.-P. Hong, J. H. Park, I. S. Choi and W. K. Cho, *Chem. Commun.*, 2014, **50**, 11649-11652.
19 Y. Ping, J. Guo, H. Ejima, X. Chen, J. J. Richardson, H. Sun and F. Caruso, *Small*, 2015, **11**, 2032-2036.
20 G. K. Such, Y. Yan, A. P. R. Johnston, S. T. Gunawan and F. Caruso, *Adv. Mater.*, 2015, **27**, 2278-2297.
21 S. Venkataraman, J. L. Hedrick, Z. Y. Ong, C. Yang, P. L. R. Ee, P. T. Hammond and Y. Y. Yang, *Adv. Drug Deliv. Rev.*, 2011, **63**, 1228-1246.
22 M. Lejars, A. Margaillan and C. Bressy, *Chem. Rev.*, 2012, **112**, 4347-4390.
23 S. H. Yang, D. Hong, J. Lee, E. H. Ko and I. S. Choi, *Small*, 2013, **9**, 178-186.
24 D. Hong, M. Park, S. H. Yang, J. Lee, Y.-G. Kim and I. S. Choi, *Trends Biotechnol.*, 2013, **31**, 442-447.
25 B. B. Hsu, K. S. Jamieson, S. R. Hagerman, E. Holler, J. Y. Ljubimova and P. T. Hammond, *Angew. Chem. Int. Ed.*, 2014, **126**, 8231-8236.
26 R. C. Smith, M. Riollano, A. Leung and P. T. Hammond, *Angew. Chem. Int. Ed.*, 2009, **48**, 8974-8977.
27 E. Vázquez, D. M. Dewitt, P. T. Hammond and D. M. Lynn, *J. Am. Chem. Soc.*, 2002, **124**, 13992-13993.
28 I. S. Choi and R. Langer, *Macromolecules*, 2001, **34**, 5361-5363.
29 M. Husemann, D. Mecerreyes, C. J. Hawker, J. L. Hedrick, R. Shah and N. L. Abbott, *Angew. Chem. Int. Ed.*, 1999, **38**, 647-649.
30 S. Kim, D. S. Kim and S. M. Kang, *Chem. Asian J.*, 2014, **9**, 63-66.
31 H. Lee, Y. Lee, A. R. Statz, J. Rho, T. G. Park and P. B. Messersmith, *Adv. Mater.*, 2008, **20**, 1619-1623.
32 M. Yu and T. J. Deming, *Macromolecules*, 1998, **31**, 4739-4745.
33 D. P. Jones, J. L. Carlson, P. S. Samiec, P. Sternberg, V. B. Mody, R. L. Reed and L. A. S. Brown, *Clin. Chim. Acta*, 1998, **275**, 175-184.
34 A. Pompella, A. Visvikis, A. Paolicchi, V. De Tata and A. F. Casini, *Biochem. Pharmacol.*, 2003, **66**, 1499-1503.
35 K. Liang, G. K. Such, Z. Zhu, Y. Yan, H. Lomas and F. Caruso, *Adv. Mater.*, 2011, **23**, H273-H277.
36 A. P. R. Johnston, G. K. Such and F. Caruso, *Angew. Chem. Int. Ed.*, 2010, **49**, 2664-2666.
37 D. C. L. Vasconcelos, V. C. Costa, E. H. M. Nunes, A. C. S. Sabioni, M. Gasparon and W. L. Vasconcelos, *Mater. Sci. Appl.*, 2011, **2**, 1375-1382.
38 R. A. Zangmeister, T. A. Morris and M. J. Tarlov, *Langmuir*, 2013, **29**, 8619-8628.
39 K. Kanazawa and N.-J. Cho, *J. Sens.*, 2009, 1-17.
40 N.-J. Cho, C. W. Frank, B. Kasemo and F. Höök, *Nat. Protoc.*, 2010, **5**, 1096-1106.
41 M. C. Dixon, *J. Biomol. Tech.*, 2008, **19**, 151-158.
42 H.-S. Lee, M. Q. Yee, Y. Y. Eckmann, N. J. Hickok, D. M. Eckmann and R. J. Composto, *J. Mater. Chem.*, 2012, **22**, 19605-19616.
43 X. Turon, O. J. Rojas and R. S. Deinhammer, *Langmuir*, 2008, **24**, 3880-3887.
44 H. Ejima, J. J. Richardson, K. Liang, J. P. Best, M. P. van Koeverden, G. K. Such, J. Cui and F. Caruso, *Science*, 2013, **341**, 154-157.
45 J. H. Park, K. Kim, J. Lee, J. Y. Choi, D. Hong, S. H. Yang, F. Caruso, Y. Lee and I. S. Choi, *Angew. Chem. Int. Ed.*, 2014, **53**, 12420-12425.